Temporal requirements of the fragile X mental retardation protein in modulating circadian clock circuit synaptic architecture

Cheryl L. Gatto and Kendal Broadie*

Department of Biological Sciences, Kennedy Center for Research on Human Development, Vanderbilt University, Nashville, TN, USA

Loss of *fragile X mental retardation 1* (*FMR1*) gene function is the most common cause of inherited mental retardation and autism spectrum disorders, characterized by attention disorder, hyperactivity and disruption of circadian activity cycles. Pursuit of effective intervention strategies requires determining when the *FMR1* product (FMRP) is required in the regulation of neuronal circuitry controlling these behaviors. In the well-characterized *Drosophila* disease model, loss of the highly conserved dFMRP causes circadian arrhythmicity and conspicuous abnormalities in the circadian clock circuitry. Here, a novel Sholl Analysis was used to quantify over-elaborated synaptic architecture in *dfmr1*-null small ventrolateral neurons (sLN$_v$s), a key subset of clock neurons. The transgenic Gene-Switch system was employed to drive conditional neuronal dFMRP expression in the *dfmr1*-null mutant background in order to dissect temporal requirements within the clock circuit. Introduction of dFMRP during early brain development, including the stages of neurogenesis, neuronal fate specification and early pathfinding, provided no rescue of *dfmr1* mutant phenotypes. Similarly, restoring normal dFMRP expression in the adult failed to restore circadian circuit architecture. In sharp contrast, supplying dFMRP during a transient window of very late brain development, wherein synaptogenesis and substantial subsequent synaptic reorganization (e.g. use-dependent pruning) occur, provided strong morphological rescue to reestablish normal sLN$_v$s synaptic arbors. We conclude that dFMRP plays a developmentally restricted role in sculpting synaptic architecture in these neurons that cannot be compensated for by later reintroduction of the protein at maturity.

Keywords: *Drosophila*, fragile X syndrome, FMRP, gene-switch, lateral neuron, pigment dispersing factor, clock circuit, synapse

INTRODUCTION

Fragile X Syndrome (FraX) is a common heritable neurological disease manifesting mental retardation, autism, attention deficit disorder and disrupted activity patterns (Bassell and Warren, 2008; Gatto and Broadie, 2009; Hagerman et al., 2009). FraX patients display characteristic hyperactivity and disordered sleep associated with altered melatonin levels (Elia et al., 2000; Gould et al., 2000; Miano et al., 2008). Similarly, FraX genetic disease models also show dramatically impaired circadian activity profiles. *Drosophila* mutants lacking their sole *fragile X mental retardation 1* (*FMR1*) family member (*dfmr1*) display significantly altered motor activity, disrupted sleep and striking circadian rhythm phenotypes, hallmarked by arrhythmicity and erratic locomotion (Dockendorff et al., 2002; Inoue et al., 2002; Morales et al., 2002; Bushey et al., 2009; Gatto and Broadie, 2009). In mammals, a tripartite gene family (*FMR1*, *FXR1* and *FXR2*) encodes proteins with >60% amino acid identity and high functional domain conservation (Siomi et al., 1995; Zhang et al., 1995). Mice deficient for either *Fmr1* or *Fxr2* alone maintain fairly normal rhythmicity, albeit with free-run periodicity shortening (Zhang et al., 2008). However, combinatorial *Fmr1/Fxr2* double null animals are entirely arrhythmic and further lack basic entrainment capacity (Zhang et al., 2008). Thus, the circadian regulation of behavior is clearly dependent on the *FMR1* gene family across a wide range of species.

The *Drosophila* circadian clock circuitry is particularly well characterized (Helfrich-Forster, 2005; Chang, 2006; Nitabach and Taghert, 2008). Within this circuit, the small ventrolateral neurons (sLN$_v$s) are a key subset of clock neurons that possess sufficient circadian pacemaker capacity to modulate morning activity peaks in light:dark cycles and drive rhythmicity in constant darkness (Renn et al., 1999; Grima et al., 2004; Stoleru et al., 2004). These critical clock neurons express the neuropeptide pigment dispersing factor (PDF) (Helfrich-Forster, 1995, 2005), which has long been proposed to serve as the clock output mediating coordination of downstream neurons. Characterization of *pdf*-null animals reveals impaired light cycle entrainment with advanced evening activity peaks and disrupted anticipation, while free-running behavior in constant darkness shows progressive deterioration of rhythmicity (Renn et al., 1999). Further, disrupted cycling of PDF within the terminal sLN$_v$ projections induced by transgenically-mediated electrical hyperexcitability causes altered behavioral rhythms with multiple periods (Nitabach et al., 2006), and work using a membrane-tethered toxin to influence neuronal ion channel properties revealed a 4-h phase advance in the PDF peak accumulation in the sLN$_v$s, which coordinately shifts morning anticipatory behavior

(Wu et al., 2008). The PDF neuropeptide facilitates circadian oscillations in individual neurons, while driving synchrony in neuronal subgroups (Sheeba et al., 2008; Yoshii et al., 2009).

Null *dfmr1* sLN$_v$s exhibit striking architectural defects, including overgrowth, overextension and mistargeting beyond the normal branching and defasiculation point in the protocerebrum, projecting a more expansive terminal synaptic arborization (Dockendorff et al., 2002; Morales et al., 2002; Reeve et al., 2005, 2008; Sekine et al., 2008; Gatto and Broadie, 2009). Conversely, targeted *dfmr1* overexpression in sLN$_v$s results in a dramatic collapse of their dorsal synaptic arbor (Reeve et al., 2005), indicating that the levels of the *dFMR1* product (dFMRP) protein alone can bidirectionally modulate synaptic complexity. Thus, dFMRP plays a critical role in controlling the synaptic connectivity within the clock circuit that drives circadian activity patterns.

A fundamental need is to determine the critical period(s) of FMRP function. Treatment design, implementation and efficacy depend upon determining whether FraX is primarily a disease of development or maintained function. FMRP has been proposed to be required very early, during neurogenesis and pathfinding, later during stages of synaptogenesis and neuronal circuitry refinement (e.g. activity-dependent synaptic pruning), or at maturity for use-dependent circuit remodeling (Nimchinsky et al., 2001; Galvez and Greenough, 2005; Larson et al., 2005; Yun et al., 2006; Bureau et al., 2008; Gatto and Broadie, 2008; Tessier and Broadie, 2008). Clearly, these potential roles may not be mutually exclusive. To distinguish these possibilities, we have used the conditional, transgenic Gene-Switch (GS) method (Osterwalder et al., 2001; Roman et al., 2001) to neuronally target wild-type dFMRP in null *dfmr1* mutants (Gatto and Broadie, 2008). Conditional expression was driven during windows throughout development and at maturity, followed by examination of the resultant sLN$_v$ synaptic architecture using a PDF-adapted modified Sholl Analysis. Neither early developmental nor adult-onset dFMRP expression was sufficient to prevent or reverse, respectively, the sLN$_v$ synaptic defects. Surprisingly, inappropriate dFMRP expression during early pupal metamorphosis actually exacerbated *dfmr1*-null phenotypes. Successful and striking structural resolution of synaptic connectivity defects was obtained only via targeted reintroduction of dFMRP during late pupal brain development. These results reveal a highly specific, dFMRP-dependent window of sLN$_v$ clock neuron development during the late stages of synaptogenesis and/or synaptic refinement.

MATERIALS AND METHODS
DROSOPHILA GENETICS
Drosophila stocks were maintained at 25°C on standard cornmeal/agar/molasses medium supplemented with yeast. The w^{1118} line served as the genetic background control for the null *dfmr1* allele (*dfmr1^{50M}*) (Zhang et al., 2001; Gatto and Broadie, 2008). Stocks carrying PDF-Gal4 and UAS-mCD8::GFP, both from the *Drosophila* Stock Center (Bloomington, IN, USA), as well as UAS-synaptotagmin-GFP (Zhang et al., 2002), were introduced into the *dfmr1*-null background using standard genetic techniques. As previously described (Gatto and Broadie, 2008), recombinant parental lines harboring the null *dfmr1* allele (Zhang et al., 2001) and either a wild-type *dfmr1* transgene under UAS control (UAS-9557-3) (Zhang et al., 2001) or the neuronal-specific driver *elav*-Gene-Switch

construct (GSG-301) (Osterwalder et al., 2001) were generated using standard genetic techniques. Accordingly, "eGS" as a genotype descriptor refers to the following: *dfmr1^{50M}*, *elav*-GSG-301/*dfmr1^{50M}*, UAS-9557-3. For RU486 (mifepristone; Sigma, St Louis, MO, USA) dosing (eGS + RU), the drug was dissolved at 10 mM in 80% ethanol (EtOH) and either mixed with food to the desired concentration for larval (0.5 μg/mL) or adult (30 μg/mL) feeding, or it was used directly for immersion treatment of both larvae and pupae as indicated. For pupal day 1 (P1) induction, late-stage wandering third instar larvae were washed briefly with EtOH, soaked in RU486 for 2 min, and then transferred to fresh vials for puparium formation. Induction from P2–P4 required an anterior incision in the pupal case with a 30-gauge needle and subsequent submersion in RU486 for 2 min. Pupae were then transferred to humid chambers to prevent desiccation. For vehicle control, equivalent volumes of 80% EtOH were used to identically treat the eGS line (eGS + E).

WESTERN BLOT ANALYSES
The central nervous system, including the brain and the ventral nerve cord, was dissected free from staged and treated larvae in Ca^{2+}-free modified standard saline, while the brain proper was dissected from both pupae and adults (Gatto and Broadie, 2008). Dissected samples were homogenized and boiled in 1X NuPage sample buffer (Invitrogen, Carlsbad, CA, USA) supplemented with 40 mM DTT. The total protein from four brains per sample was loaded onto 4–12% Bis-Tris gels and electrophoresed in NuPage MES Buffer (Invitrogen) for 1 h at 200 V. Transfer to nitrocellulose was carried out for 1 h at 100 V in NuPage transfer buffer (Invitrogen) with 10% MeOH. Processing was completed using the Odyssey near infrared fluorescence detection system (Li-COR, Lincoln, NE) to enable quantitative Western blot analysis. Antibodies used included: anti-dFMRP (1:2000; 6A15 monoclonal, Sigma), anti-α-tubulin (1:200,000; B512 monoclonal, Sigma), and Alexa-goat-anti-mouse-680 (1:10,000; Invitrogen-Molecular Probes). Raw integrated intensities were calculated for the lower molecular weight band of the dFMRP doublet and for the α-tubulin band. The ratio of dFMRP:α-tubulin normalized for loading and allowed comparison of eGS neuronally induced dFMRP relative to endogenous dFMRP in age matched wild-type (w^{1118}) animals.

IMMUNOHISTOCHEMISTRY
Immunohistochemistry was performed essentially as previously described (Gatto and Broadie, 2008). Brains from staged and treated animals (0–3 days old) were dissected in standard saline and then fixed for 40 min with 4% paraformaldehyde/4% sucrose in phosphate buffered saline (PBS), pH 7.4. Preparations were rinsed with PBS, then blocked and permeablized with 0.2% triton X-100 in PBS (PBST) supplemented with 1% bovine serum albumin (BSA) and 0.5% normal goat serum (NGS) for 1 h at room temperature. Primary and secondary antibodies were diluted in PBST with 0.2% BSA and 0.1% NGS and incubated overnight at 4°C and 2 h at room temperature, respectively. Antibodies employed include: anti-GFP (1:2000; ab290 polyclonal, Abcam Inc., Cambridge, MA), anti-PDF [1:5; C7 monoclonal, Developmental Studies Hybridoma Bank (DSHB), University of Iowa], anti-ELAV (1:100; 9F8A9 monoclonal, DSHB), anti-dFMRP (1:500; 6A15, Sigma) and Alexa-Fluor secondaries (1:250; Invitrogen-Molecular Probes). All fluorescent

images were collected using a ZEISS LSM 510 META laser scanning confocal microscope.

PDF-ADAPTED MODIFIED SHOLL ANALYSIS

A PDF-adapted version of the Modified Sholl Analysis (Fernandez et al., 2008) was developed. A traditional Sholl array using a series of 10 μm-spaced concentric rings was centered upon the dorsal horn bifurcation of the sLN_v terminal arbor and extended forward for 100 μm with assays conducted at *zeitgeber time* 2–4, i.e. 2–4 h after lights on. To provide for compatibility with the GS system, this assay examined PDF reactive puncta (≥1 μm in diameter) within each 10 μm concentric ring. Puncta were counted as a reflective index of spatial synaptic arbor complexity. Values were determined for each concentric ring throughout the arbor in both left and right hemispheres and averaged for $n = 1$ for each individual animal.

STATISTICS

Statistical analyses were performed using GraphPad InStat 3 (GraphPad Software, Inc., San Diego, CA, USA). Unpaired, nonparametric, two-tailed Mann–Whitney tests were used to compare means of control and *dfmr1*, as well as means of eGS treated with vehicle or RU486 in the PDF-adapted Modified Sholl Analysis. While unpaired, parametric student's *t*-tests could have been applied in certain instances, the cumulative consideration of data sets examining each concentric ring in a given treatment paradigm did vary with regard to normality. Thus, it was deemed more appropriate to globally apply the more conservative, nonparametric measures. Significance levels in figures are represented as $p < 0.05$ (*); $p < 0.01$ (**); $p < 0.001$ (***). All error bars represent standard error of the mean (SEM).

RESULTS

OVER-ELABORATION OF sLN_v SYNAPTIC ARBORS IN *dfmr1*-null MUTANTS

In the *Drosophila* FraX model, dFMRP loss results in overgrowth of sLN_v synaptic arbors in the dorsal brain (Dockendorff et al., 2002; Morales et al., 2002; Reeve et al., 2005, 2008; Sekine et al., 2008; Gatto and Broadie, 2009). The increased architectural complexity can be readily visualized with expression of the UAS-mCD8::GFP membrane marker transgene driven by the LN_v-specific PDF-GAL4, comparing control and *dfmr1*-null mutant (**Figure 1A**). Co-immunostaining for the LN_v-specific neuropeptide PDF reveals a punctate pattern of varicosities distributed throughout the sLN_v synaptic arbor interspersed along the axonal branches. Likewise, expression of the UAS-synaptotagmin-GFP transgene, an integral synaptic vesicle marker, specifically labels synaptic boutons within the sLN_v arbor revealing the same characteristic synaptic overgrowth in *dfmr1*-null mutants (**Figure 1B**). Double-labeling shows an array of synaptotagmin-GFP boutons within the synaptic arbor, overlapping and co-localized with the anti-PDF array. These analyses show that PDF labeling serves as an excellent indicator of synaptic boutons in both control and *dfmr1* nulls (**Figure 1B**). Co-localization of PDF with synaptotagmin-GFP was seen in 77 ± 3% of puncta in control and 71 ± 2% in *dfmr1* mutants ($p = 0.13$, $n = 7$ for both). PDF was independently present in 19 ± 3% of control puncta vs. 23 ± 2% in *dfmr1* ($p = 0.21$), and synaptotagmin-GFP was observed alone in 4 ± 1% of control and 6 ± 0.3% of *dfmr1* puncta ($p = 0.13$).

We conclude that examining the spatial distribution of PDF puncta serves as a reflective index of both the axonal arbor morphological complexity and synaptic bouton distribution in the sLN_vs.

To quantify the synaptic defects in *dfmr1* mutants, we employed a PDF-adapted modified Sholl Analysis to record sLN_v synapse architecture (**Figure 1C**, inset) (Fernandez et al., 2008). The approach involves aligning a traditional Sholl array of 10 μm-spaced concentric rings centered upon the dorsal horn bifurcation of the sLN_v terminal arbor, extending the array for 100 μm, and reporting the number of PDF synaptic boutons within each ring. This method reliably characterizes the robust differential distribution of synaptic boutons in *dfmr1* mutants compared to control (**Figure 1C**). These quantified analyses reveal that *dfmr1*-null animals harbor increased numbers of synaptic boutons throughout the sLN_v terminal (total puncta: 51 ± 4 control vs. 92 ± 5 *dfmr1*; $n = 26$ for both; $p < 0.0001$) projecting, at minimum, 20 μm further toward the midline (average maximal ring occupancy: 6 ± 0.2 control vs. 8 ± 0.3 *dfmr1*; $p < 0.0001$) and with a greatly increased average number of boutons beyond 50 μm (3 ± 1 control vs. 16 ± 3 *dfmr1*; $p < 0.0001$). Moreover, the number of synaptic boutons in every concentric ring is significantly elevated in *dfmr1* nulls throughout the arbor (**Figure 1C**): 10 μm ring (11 ± 1 control, 14 ± 1 *dfmr1*; $p = 0.039$), 20 μm ring (15 ± 1 control, 19 ± 1 *dfmr1*; $p = 0.004$); 30 μm ring (11 ± 1 control, 16 ± 1 *dfmr1*; $p = 0.0001$), 40 μm ring (8 ± 1 control, 15 ± 1 *dfmr1*; $p < 0.0001$), 50 μm ring (3 ± 0.5 control, 12 ± 1 *dfmr1*; $p < 0.0001$), 60 μm ring (2 ± 0.5 control, 7 ± 1 *dfmr1*, $p < 0.0001$), 70 μm ring (1 ± 0.3 control, 4 ± 0.7 *dfmr1*; $p < 0.0001$), 80 μm ring (0.3 ± 0.1 control, 2 ± 0.5 *dfmr1*; $p = 0.002$), 90 μm ring (0.04 ± 0.04 control, 2 ± 0.6 *dfmr1*; $p = 0.023$), and the most distal 100 μm ring (0 control, 1 ± 0.4 *dfmr1*). These results show that both the number and spatial distribution of boutons in the sLN_v synaptic arbor is altered in the absence of dFMRP, with more boutons occupying a larger territory beyond the normal extent of the sLN_v arborization.

GENE-SWITCH CONDITIONAL CONTROL OF dFMRP DURING DEVELOPMENT AND AT MATURITY

To examine the temporal requirement(s) of dFMRP in regulating synapse architecture and to determine whether dFMRP reintroduction could rescue synaptic defects, we exploited the transgenic conditional GS system (Osterwalder et al., 2001; Roman et al., 2001). The GS method employs a hormone-responsive modified UAS-GAL4 system to drive inducible, targeted, tissue-specific transgene expression. We controlled a UAS-*dfmr1* transgene with the pan-neuronal *elav*-GS GAL4 by treating with the activating progesterone analog, RU486 (mifepristone), in the *dfmr1*-null mutant background to examine the influence of dFMRP reintroduction on sLN_v morphology and synaptic elaboration (**Figure 1**) (Gatto and Broadie, 2008). In defining treatment paradigms, analyses were performed on wild-type control (w^{1118}), *dfmr1*-null and *dfmr1*-null animals harboring both the *elav*-GS GAL4 driver and UAS-*dfmr1* transgene (eGS animals, henceforth) treated with RU486 (eGS + RU) or only ethanol vehicle (eGS + ET) as indicated (**Figure 2A**). We first confirmed that RU486 induced *elav*-GS GAL4 does drive dFMRP transgene expression pan-neuronally in the brain, albeit not uniformly (**Figure 2A**). Close examination likewise confirmed elav expression in the sLN_vs nuclei (**Figure 2B**), establishing that sLN_vs
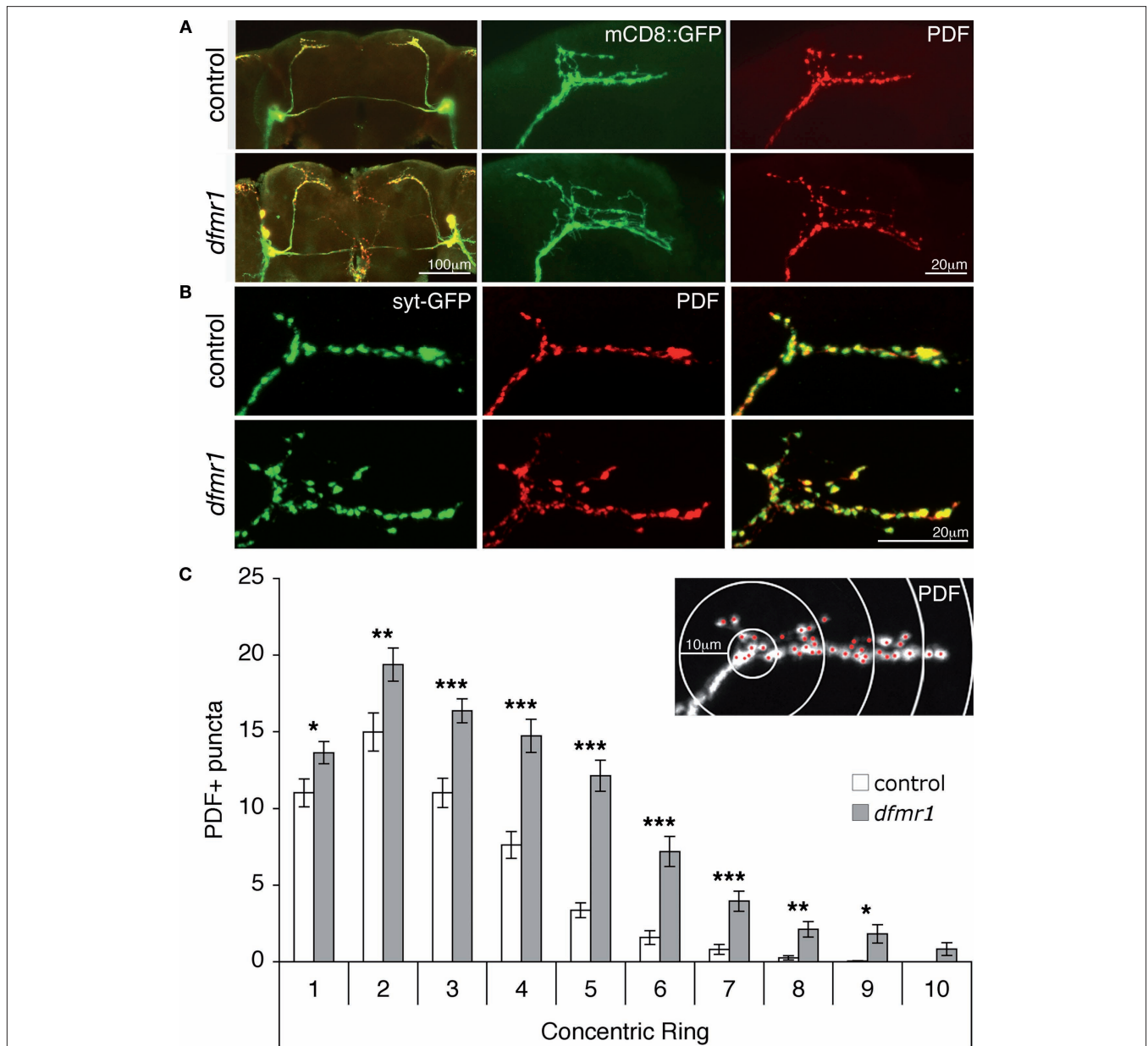
FIGURE 1 | sLN$_v$ synaptic architecture defects in the absence of dFMRP.
(A) Representative images of adult *Drosophila* brains isolated from animals expressing a UAS-mCD8::GFP (green) transgene under the control of the ventrolateral neuron (LN$_v$) specific PDF-GAL4 driver in both genetic background control and homozygous *dfmr1^{50M}* null (*dfmr1*) mutants. Co-immunohistochemistry was done for the LN$_v$ neuropeptide PDF (red). At left, low magnification images show both the large LN$_v$ axonal projections with the established posterior optic tract connecting both hemispheres and the small LN$_v$ (sLN$_v$) axonal tracts that defasiculate and arborize in the protocerebrum. At right,
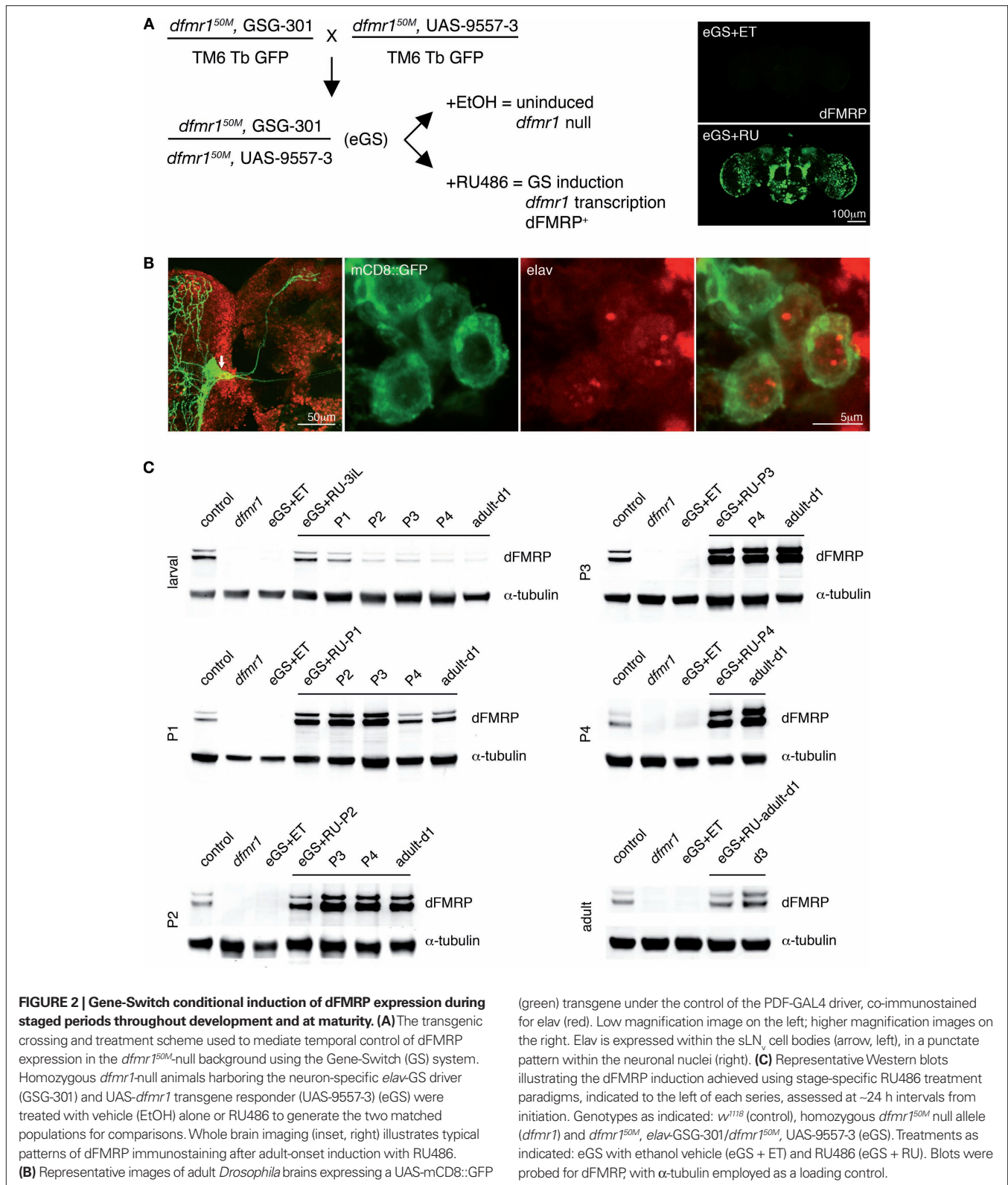
high magnification views focus solely on the terminal sLN$_v$ synaptic arbors. **(B)** Images of sLN$_v$ synaptic arbors from animals expressing UAS-synaptotagmin-GFP (syt-GFP, green) under the control of PDF-GAL4 in both control and *dfmr1*-null backgrounds. Brains show co-immunohistochemistry for PDF (red). **(C)** Sholl Analysis quantification of the spatial distribution of synaptic boutons throughout the sLN$_v$ arbor in both genetic background controls and *dfmr1* nulls based on counting PDF-reactive (PDF+) puncta (inset; ≥1 μm in diameter, demarcated in red) starting from the point of dorsal horn bifurcation. Bars indicate mean ± SEM Significance levels: $p < 0.05$ (*); $p < 0.01$ (**); $p < 0.001$ (***).

are elav-positive. These findings indicate that the GS method allows control of dFMRP expression in neurons widely throughout the brain, including within the sLN$_v$ neurons.

The expression of dFMRP is strongly modulated as a function of age both during development and adult aging, with peak expression at the late stages of brain maturation (Gatto and Broadie, 2008; Tessier

and Broadie, 2008; Bushey et al., 2009). Therefore, RU486 treatment windows were assessed at all time points during development and at maturity for both endogenous and induced dFMRP expression levels (**Figure 2C**). Progressive interventions were performed to drive dFMRP transgene expression from the earliest stages of development, through intermediate and later stages, culminating with adult-onset

FIGURE 2 | Gene-Switch conditional induction of dFMRP expression during staged periods throughout development and at maturity. (A) The transgenic crossing and treatment scheme used to mediate temporal control of dFMRP expression in the *dfmr1⁵⁰ᴹ*-null background using the Gene-Switch (GS) system. Homozygous *dfmr1*-null animals harboring the neuron-specific *elav*-GS driver (GSG-301) and UAS-*dfmr1* transgene responder (UAS-9557-3) (eGS) were treated with vehicle (EtOH) alone or RU486 to generate the two matched populations for comparisons. Whole brain imaging (inset, right) illustrates typical patterns of dFMRP immunostaining after adult-onset induction with RU486. **(B)** Representative images of adult *Drosophila* brains expressing a UAS-mCD8::GFP

(green) transgene under the control of the PDF-GAL4 driver, co-immunostained for elav (red). Low magnification image on the left; higher magnification images on the right. Elav is expressed within the sLN$_v$ cell bodies (arrow, left), in a punctate pattern within the neuronal nuclei (right). **(C)** Representative Western blots illustrating the dFMRP induction achieved using stage-specific RU486 treatment paradigms, indicated to the left of each series, assessed at ~24 h intervals from initiation. Genotypes as indicated: w^{1118} (control), homozygous *dfmr1⁵⁰ᴹ* null allele (*dfmr1*) and *dfmr1⁵⁰ᴹ*, *elav*-GSG-301/*dfmr1⁵⁰ᴹ*, UAS-9557-3 (eGS). Treatments as indicated: eGS with ethanol vehicle (eGS + ET) and RU486 (eGS + RU). Blots were probed for dFMRP, with α-tubulin employed as a loading control.

expression. The earliest induction was to constitutively feed RU486 throughout larval development (instars 1–3) and then remove animals from treatment. Controlled RU486 dosage was used to match endogenous dFMRP levels, measured in wandering third instar larvae

at $94 \pm 11\%$ ($n = 3$) of the corresponding control levels (**Figure 2C**). Following removal of the drug, dFMRP level rapidly declined during pupal stages (P1–P4) and was almost entirely absent by eclosion into the adult allowing transient early dFMRP expression.

Sequential RU486 treatments were used during each day of pupal metamorphosis to drive dFMRP expression starting at pupal day 1 (P1), P2, P3 and P4 (**Figure 2C**). Induction at P1 was achieved by bath application of RU486 on the late wandering third instar larvae, just prior to puparium formation. This treatment drives dFMRP expression starting in P1 and extending into the early stages of pupal development (**Figure 2C**). We previously reported a quantified half-life of dFMRP driven by larval RU486 induction of ~25 h (Gatto and Broadie, 2008). In the pupae, induced dFMRP persists longer, presumably owing to restrictions on drug clearance and metabolism in the pupae, so that pupal RU486 treatments result in broader windows of expression. In each of the later pupal interventions, the pupal case cuticle was cut to introduce RU486 via brief (2 min) bath application for absorption (**Figure 2C**). Treatments were performed just prior to the onset of day P2, P3 and P4 to drive dFMRP expression, which was then monitored over subsequent 24 h intervals progressing to adult eclosion.

The final intervention was to drive dFMRP expression only at maturity in an otherwise *dfmr1*-null mutant condition. Larvae and pupae were reared until eclosion in the absence of RU486, and no dFMRP expression was detectable (**Figure 2C**). Following eclosion, adult animals were then fed RU486 to drive dFMRP levels matching wild type after 24 h of treatment. Adult onset expression was maintained for an additional 72 h course to assess the consequences of continued adult dFMRP expression (**Figure 2C**).

EARLY DEVELOPMENTAL AND ADULT-ONSET dFMRP EXPRESSION DO NOT ALLEVIATE *dfmr1*-null DEFECTS

Using the conditional GS system, we systematically investigated when reintroduction of dFMRP could restore the gross sLN$_v$ synaptic architecture defects of the *dfmr1* null (**Figure 1**). We examined how each inductive paradigm might modulate synaptic structure, as quantified with our modified Sholl Analysis of synaptic bouton spatial distribution (**Figure 1C**). We first examined animals in which normal dFMRP levels were driven throughout larval life, the period of neurogenesis and neural fate specification. This developmentally early intervention provided no detectable restorative effect on the organization of the sLN$_v$s arborization or synaptic bouton disposition as compared to the eGS + ET animals, which phenocopy the *dfmr1* null alone (**Figure 3A**). When dFMRP is introduced during larval stages only, the resultant adults display PDF puncta within the sLN$_v$ arbors that remain unchanged with respect to total number (eGS + ET: 88 ± 6, $n = 10$ vs. eGS + RU: 85 ± 6, $n = 10$; $p = 0.97$) and spatial distribution throughout the Sholl array (**Figure 3A**, right). We conclude that providing dFMRP transiently during early stages of neural development provides no benefit for correcting the hallmark synaptic defects caused by the loss of dFMRP as assayed at maturity.

We next assayed whether adult-onset dFMRP induction could rescue synaptic defects in *dfmr1*-null animals (**Figure 3B**). This determination is particularly important for the design of FraX intervention strategies, as it addresses the question of whether the synaptic overgrowth characteristic of the disease is reversible at a state of maturity. eGS *dfmr1*-null animals were raised in the absence of RU486 induction preventing dFMRP expression during development and then switched to an RU486-containing diet at eclosion. eGS animals with sustained induction for the following 3 days showed no detectable reversal of the overgrown sLN$_v$ synaptic

terminal area, the over-elaborated synaptic branch arborization, or the over-proliferation of synaptic boutons as compared to the eGS + ET animals, which phenocopy the *dfmr1* null alone (**Figure 3B**). When reintroduced only in the adult, the aged adult animals expressing dFMRP display PDF synaptic puncta within the sLN$_v$s arbors that remain unchanged with respect to total number (eGS + ET: 77 ± 4, $n = 15$ vs. eGS + RU: 73 ± 4, $n = 15$; $p = 0.63$) and spatial distribution throughout the Sholl array (**Figure 3B**, right). We conclude that providing dFMRP at maturity, following completion of neural development, provides no benefit for correcting the hallmark synaptic defects caused by the loss of dFMRP.

Despite reintroduction of dFMRP throughout either the larval or adult phase, no palliative effect was observed in the *dfmr1*-null sLN$_v$ synaptic connections. Therefore, we next tested whether phenotypic reversal of these defects would be identifiable upon dFMRP elevation in these cells. We compared two conditions: (1) UAS-mCD8:: GFP alone, and (2) UAS-mCD8::GFP co-expressed with UAS-*dfmr1*, specifically driven in sLN$_v$s (**Figure 3C**). dFMRP in the control is expressed at a uniform low level in neurons, including the sLN$_v$ clock neurons (**Figure 3C**, top row, red), whereas targeted dFMRP, exploiting the PDF-GAL4 driver, elevates expression only in these cells (**Figure 3C**, middle row, red, arrows). This targeted, constitutive expression of dFMRP within the sLN$_v$s results in collapse and retraction of the terminal synaptic arbor, evident in the reduction of synaptic area encompassed, loss of synaptic varicosities and complete lack of outward projecting axonal branches (**Figure 3C**, green). Examination of the PDF distribution within these collapsed terminal arbors revealed that, although the gross anatomy of the synapse was radically altered, discrete PDF-positive synaptic puncta remained apparent (**Figure 3C**, bottom row, red). These results suggest that the presynaptic potential of the sLN$_v$s remains intact. In contrast to the changes resulting from constitutive lateral neuron-specific dFMRP overexpression, timed pan-neuronal dFMRP introduction with the GS system, either early or late, causes no such change in the synaptic arborization of the *dfmr1* null sLN$_v$s, which remain over-extended and over-elaborated. Even over-expression of dFMRP in the adult (**Figures 2A,C**, after full 72 h RU486 treatment: 246 ± 14% control level, $n = 4$) failed to cause a reduction in the synaptic arbor of the null mutant, showing that the over-expression effect is likewise restricted to a specific developmental window. These results together strongly suggest that GS-induced dFMRP expression has not yet been provided at the appropriate stage.

A CRITICAL WINDOW OF dFMRP REQUIREMENT DURING LATE BRAIN DEVELOPMENT

The above results suggest that the requirement for dFMRP function in synaptic patterning likely occurs in the period of late brain development during pupal metamorphosis. This timing is consistent with elevated endogenous dFMRP expression during the late pupal period, and the role of dFMRP during this period in activity-dependent synaptic refinement (Tessier and Broadie, 2008). As the pupal period lasts 4 days at 25°C (P1–P4), we subdivided this period by inducing dFMRP at the start of each consecutive day in turn in otherwise *dfmr1*-null mutant animals (**Figure 2B**). The consequences on sLN$_v$ clock neuron synaptic arborizations were then evaluated in mature adults (d1–2) in each case. The results of these studies are shown in **Figure 4**.
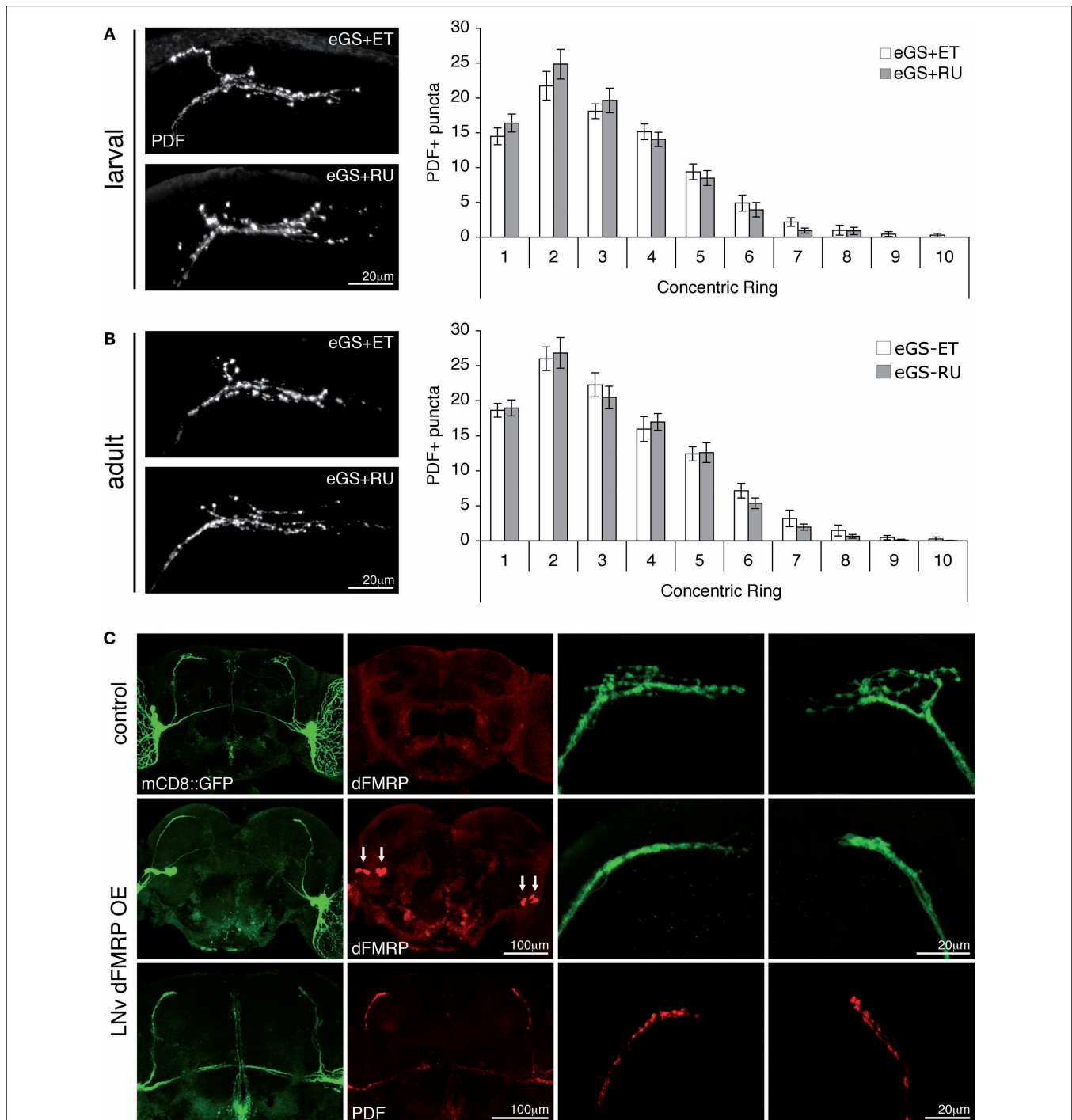
FIGURE 3 | dFMRP induction during early development and at maturity provides no rescue of *dfmr1*-null mutant sLN$_v$ defects. (A) Comparison of the *dfmr1*-null eGS ethanol vehicle (eGS + ET) and RU486 (eGS + RU) treatment throughout larval development (instars L1–L3). At left, representative images shown of adult sLN$_v$ terminal arbors immunostained for PDF. At right, quantification from the Sholl Analysis indicating no change with RU486 induction. **(B)** Analyses of adult-onset dFMRP induction. At left, representative images shown from control and RU486-induced animals (treated d1–3) with sLN$_v$ synaptic arbors immunostained for PDF. At right, quantification from the Sholl Analysis indicating no change with RU486 induction. **(C)** Representative images of ventrolateral clock neurons expressing either UAS-mCD8::GFP (green) alone under the control of PDF-GAL4 (control: PDF-GAL4/UAS-mCD8::GFP) or in conjunction with, and thus overexpressing, UAS-*dfmr1* (LNv dFMRP OE: PDF-GAL4/UAS-mCD8::GFP; UAS-9557-3, *dfmr1^{50M}/+*). Co-immunolabeling for dFMRP (red) illustrates endogenous (top row) and transgenic (middle row) levels in the brain, and specifically in the sLN$_v$ cell bodies (arrows). High magnification views illustrate the sLN$_v$ synaptic arbor collapse caused by cell-autonomous over-expression of dFMRP. Examination of collapsed arbors via co-immunolabelling for PDF (red, bottom row) revealed the persistence of PDF-positive presynaptic boutons.
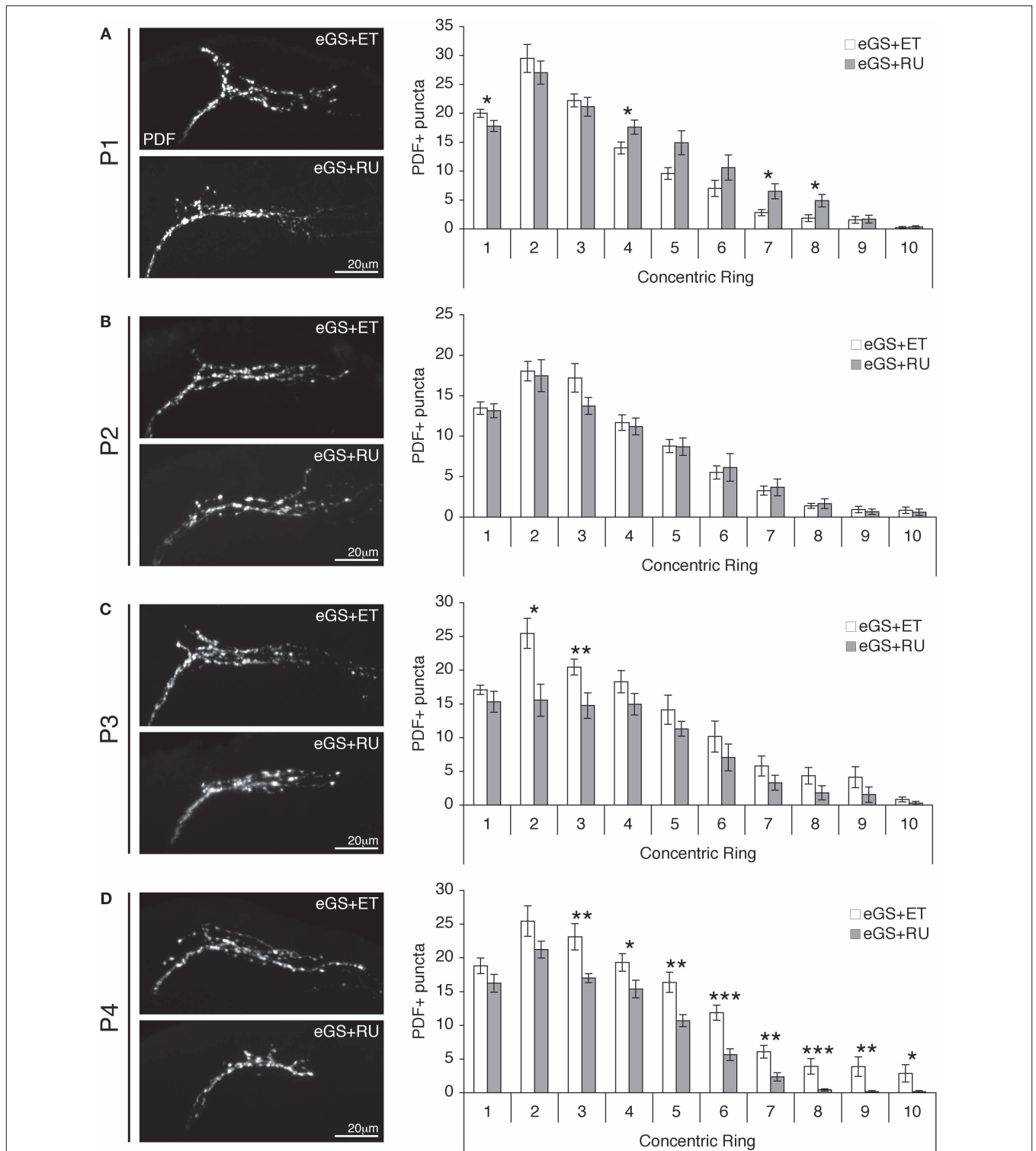
FIGURE 4 | dFMRP induction only during late brain maturation restores normal sLN_v synaptic architecture. (A) Representative images of adult sLN_v synaptic arbors immunostained for PDF after pupal day 1 (P1) inductive treatment with ethanol vehicle (eGS + ET) or RU486 (eGS + RU). At right, quantification from the PDF-adapted modified Sholl Analysis, indicating a moderately exacerbated mutant phenotype. Significance levels: $p < 0.05$ (*). **(B)** Representative images of adult sLN_v synapses immunostained for PDF after P2 inductive treatment with ethanol vehicle (eGS + ET) or RU486 (eGS + RU). At right, quantification showing no change with dFMRP induction. **(C,D)** Representative images are displayed of adult sLN_v terminal synapses immunostained for PDF after P3 **(C)** or P4 **(D)** treatment with ethanol vehicle (eGS + ET) or RU486 (eGS + RU). Quantifications show significant rescue of the synaptic defects. Significance levels: $p < 0.05$ (*); $p < 0.01$ (**); $p < 0.001$ (***).

We began with RU486 drug delivery to drive dFMRP induction at the earliest stage of pupal development, with induction at pupal day 1 (P1; **Figure 4A**). This early phase dFMRP expression provided no correction of the *dfmr1*-null sLN$_v$ synapses compared to the eGS + ET animals, which phenocopy the *dfmr1* null alone. Indeed, this inappropriate early induction exacerbated the mutant phenotype, resulting in an elevated number of PDF synaptic boutons redistributed within 30% of the sLN$_v$ axonal arbor based on the Sholl Analysis (**Figure 4A**, right). While the total number of boutons was unchanged ($p = 0.32$; $n = 11$ eGS + ET, $n = 14$ eGS + RU), the spatial distribution of boutons was significantly altered, with an increased number of boutons in the 40 μm concentric ring (eGS + ET: 14 ± 1 vs. eGS + RU: 18 ± 1; $p = 0.025$), 70 μm ring (eGS + ET: 3 ± 0.5 vs. eGS + RU: 7 ± 1; $p = 0.037$), and 80 μm ring (eGS + ET: 2 ± 0.6 vs. eGS + RU: 5 ± 1; $p = 0.035$). The overall frequency of boutons in the more distal domains was shifted from 82% to 93% at 70 μm and from 63% to 93% at 80 μm in eGS + ET compared to eGS + RU (**Figure 4A**, right). Similarly, induction at P2 provided no improvement of the *dfmr1*-null sLN$_v$ architecture compared to the eGS + ET animals (**Figure 4B**). P2 induction of dFMRP provided no significant influence upon the synaptic arborization, with no change in the total number of PDF boutons (eGS + ET: 81 ± 4, $n = 15$ vs. eGS + RU: 77 ± 7, $n = 15$; $p = 0.27$) or their spatial distribution (**Figure 4B**, right). We conclude that induction of dFMRP during the first half of pupal development does not restore normal synaptic connectivity in the null mutant animals.

In contrast to all of the preceding interventions, reintroduction of dFMRP specifically within the latter half of pupal development provided the key to structural reparation of the *dfmr1*-null sLN$_v$ synaptic defects. At P3, dFMRP induction resulted in partial rescue of the synaptic arbor, including the number of synaptic boutons and the extent of spatial overgrowth (**Figure 4C**, left). Based on the Sholl Analysis, there was a highly significant reduction in the total number of PDF boutons present in the synaptic terminal arbor ($p = 0.009$; $n = 12$ eGS + ET, $n = 10$ eGS + RU), with the restoration effect most pronounced in the region immediately adjacent to the dorsal horn bifurcation (**Figure 4C**, right). PDF-reactive boutons were reduced in both the 20 μm concentric ring (eGS + ET: 25 ± 2, vs. eGS + RU: 16 ± 2; $p = 0.013$) and the 30 μm domain (eGS + ET: 20 ± 1 vs. eGS + RU: 15 ± 2; $p = 0.007$). The most dramatic rescue was effected upon dFMRP induction at the very end of development, during pupal day 4 (P4; **Figure 4D**). Throughout the sLN$_v$ synaptic arbors the total number of PDF boutons was very significantly reduced ($p < 0.0001$; $n = 12$ eGS + ET, $n = 15$ eGS + RU), with spatially specific resolution achieved over more than 80% of the arbor area (**Figure 4D**, right). The distal concentric rings from 30 to 100 μm displayed the following decrements in PDF boutons: 30 μm (eGS + ET: 23 ± 2 vs. eGS + RU: 17 ± 1, $p = 0.003$), 40 μm (eGS + ET: 19 ± 1 vs. eGS + RU: 15 ± 1, $p = 0.026$), 50 μm (eGS + ET: 16 ± 2 vs. eGS + RU: 11 ± 1, $p = 0.004$), 60 μm (eGS + ET: 12 ± 1 vs. eGS + RU: 6 ± 1, $p = 0.0006$), 70 μm (eGS + ET: 6 ± 1 vs. eGS + RU: 2 ± 1, $p = 0.005$), 80 μm (eGS + ET: 4 ± 1 vs. eGS + RU: 0.4 ± 0.2, $p = 0.0004$), 90 μm (eGS + ET: 4 ± 1 vs. eGS + RU: 0.2 ± 0.2, $p = 0.001$) and 100 μm (eGS + ET: 3 ± 1 vs. eGS + RU: 0.2 ± 0.2, $p = 0.011$). We conclude that dFMRP plays a highly specific role in the very latest stages of synaptic development

and refinement that is required to properly restrict the number and specificity of synaptic connections, and that dFMRP is capable of operating in this mechanism only during this strictly defined developmental window of opportunity.

DISCUSSION

Loss of FMRP compromises the synaptic connectivity of the circadian clock circuit and impairs the behavioral output of rhythmic circadian activity patterns, making this system ideal for investigating the temporal requirements for FMRP function (Elia et al., 2000; Gould et al., 2000; Dockendorff et al., 2002; Inoue et al., 2002; Morales et al., 2002; Reeve et al., 2005, 2008; Miano et al., 2008; Sekine et al., 2008; Zhang et al., 2008; Bushey et al., 2009). Using our well-established *Drosophila* FraX model (Zhang et al., 2001; Bolduc et al., 2008; Gatto and Broadie, 2008; Pan et al., 2008; Tessier and Broadie, 2008; Repicky and Broadie, 2009) and the well-characterized *Drosophila* clock circuitry (Helfrich-Forster, 2005; Chang, 2006; Nitabach and Taghert, 2008), this study was aimed at identifying the critical period(s) of dFMRP function in the synaptic organization of clock neurons. The GS method provides tight temporal control of transgene expression specifically within neurons (Osterwalder et al., 2001; Roman et al., 2001), allowing us to dissect the exact timing of the dFMRP requirement. We have identified a single responsive time window, pupal days 3–4, during which reintroduction of dFMRP provides rescue of the arbor overgrowth and excessive synapse establishment characterizing the *dfmr1*-null mutant. Introduction of dFMRP either before or after this period provides no benefit. We conclude, therefore, that dFMRP function in sculpting synaptic connections is locked into this transient developmental time window. As these studies were conducted with pan-neuronal expression, we cannot yet distinguish between a cell autonomous function of dFMRP in sLN$_v$ clock neurons compared to potential roles of dFMRP in neighboring neurons.

We have previously investigated the temporal requirements of dFMRP at the peripheral glutamatergic neuromuscular junction (NMJ) (Gatto and Broadie, 2008). In *dfmr1*-null mutants, this synaptic arbor is over-elaborated with expanded synaptic area, excess synaptic branching and supernumerary synaptic boutons (Zhang et al., 2001), thus closely resembling the phenotype in the central brain clock neurons shown here. Employing GS inductive paradigms to drive dFMRP in the *dfmr1*-null mutant background, these studies similarly demonstrate a temporally restricted role for dFMRP in sculpting synaptic architecture (Gatto and Broadie, 2008). Re-introduction of dFMRP only during the period of normal NMJ synaptogenesis enabled the correct development and maintenance of standard, sustainable terminal structure. In contrast, dFMRP introduction at maturity provided very little rescue of the mutant overgrown synaptic defects, with only weak, partial reduction in the number of synaptic boutons (Gatto and Broadie, 2008). The partial rescue achieved likely reflects the fact that synaptogenesis continues throughout the larval period in *Drosophila*, and therefore development and maturity are not as well separated as in the brain clock circuit. Overall, these previous findings at the NMJ strongly support our current results of a transient development requirement for dFMRP within the sLN$_v$ clock neurons.

Interestingly, a host of FraX-associated phenotypes are known to be developmentally transient, also suggesting temporally-restricted

FMRP function. In the *Drosophila* FraX model, *dfmr1*-null mushroom body neurons display heightened axonal and dendritic complexity, with excessive synaptic connectivity (Pan et al., 2004). These defects become evident only very late in pupal brain development, with the appearance of abnormally long axonal branches and associated excessive synaptic processes (Tessier and Broadie, 2008). Upon initial use following eclosion, activity-dependent synaptic pruning occurs in wild-type but completely fails in *dfmr1*-null mutant neurons. Following this normal dFMRP-dependent developmental window, delayed and inappropriate pruning occurs in the absence of dFMRP (Tessier and Broadie, 2008). This refinement process takes days in *Drosophila*, but occurs over the course of weeks in mice. Similar to the *Drosophila* findings, in *Fmr1*-null mouse layer V somatosensory barrel cortex, the increase in synaptic dendrite spine length and density manifests during postnatal week 1, attenuates by week 2 and is undetectable by week 4 (Nimchinsky et al., 2001; Galvez and Greenough, 2005). Likewise, *Fmr1*-null ascending projections connecting layers III and IV display aberrant transmission strength, experience-dependent plasticity and axonal arborization at postnatal week 2, which also resolves by postnatal week 3–4 (Bureau et al., 2008). These studies suggest a transient FMRP role in synaptic development and refinement. It should be noted that differences could yet arise between the *Drosophila* and murine FraX models with regard to the temporal requirements for FMRP. Mice harbor the two *Fmr1* paralogs, *Fxr1* and *Fxr2* (Siomi et al., 1995; Zhang et al., 1995), which could influence the effects of *Fmr1* deletion during development. However, the protracted postnatal period required for circuit refinement in mammals needs to be carefully considered to define developmental vs. adult FMRP requirement. We eagerly await the establishment of similar mouse conditional *Fmr1* expression models to provide further insight into the etiology of FraX.

In the *Drosophila* FraX model, the P3–P4 critical period definition for sLN$_v$ synaptic structuring is entirely consistent with our recent finding that dFMRP levels are transiently elevated during this same period (Tessier and Broadie, 2008), with subsequent rapid decrement following maturation (Tessier and Broadie, 2008; Bushey et al., 2009). A similar transient period of FMRP elevation is reported in rodents, likewise corresponding to the restricted period of synaptogenesis and synaptic refinement (Khandjian et al., 1995; Singh et al., 2007; Singh and Prasad, 2008). During the corresponding period, dFMRP has been shown to regulate a similar stage-dependent mechanism of activity-dependent axonal pruning and synapse elimination in the *Drosophila* mushroom body (Tessier and Broadie, 2008). Assuming a conserved mechanism within the clock circuit, this role would explain the temporally-restricted dFMRP function in establishing appropriate sLN$_v$ synaptic connections. Consistent with this transient critical window for dFMRP function, assays to ameliorate *dfmr1*-null clock defects by decreased metabotropic glutamate receptor (mGluR) signaling, via treatment with mGluR antagonists such as 2-methyl-6-phenylethynyl-pyridine (MPEP), fail to resolve circadian impairments with treatment either during larval development or in the adult (McBride et al., 2005). We suggest that such previous pharmacological treatment attempts have inadvertently missed the therapeutic target window of late brain development.

FMRP is an RNA-binding, polysome-associated protein that influences mRNA trafficking/stability (Zalfa et al., 2005; Zhang et al., 2007; Dictenberg et al., 2008; Estes et al., 2008) and regulates protein translation (Laggerbauer et al., 2001; Li et al., 2001; Sung et al., 2003; Zalfa et al., 2003; Lu et al., 2004; Qin et al., 2005; Tessier and Broadie, 2008; Bechara et al., 2009). In the *Drosophila* brain, dFMRP negatively regulates cytoskeleton organizing proteins such as Futsch, the mictrobule-binding MAP1B homolog, and Chickadee, the actin-binding Profilin homolog (Zhang et al., 2001; Reeve et al., 2005; Tessier and Broadie, 2008). In sLN$_v$ clock neurons, overexpression of Chickadee mimics *dfmr1*-null architectural defects, while concurrently decreasing Chickadee levels in the *dfmr1* null suppresses the phenotypes (Reeve et al., 2005). Importantly, *dfmr1* mutants display only a developmentally transient elevation of Chickadee expression at P4 into post-eclosion day 1 (Tessier and Broadie, 2008). Thus, targeted reintroduction of dFMRP at this time point would prevent the elevated protein levels, providing for normal synaptic architecture and connectivity. In parallel, dFMRP also modulates the actin cytoskeleton by regulating the small GTPase Rac1 (Lee et al., 2003), CYFIP/Sra-1 (cytoplasmic FMRP interacting protein) (Schenck et al., 2003) and the actin depolymerizing factor/Cofilin (Castets et al., 2005; Le Clainche and Carlier, 2008), which all may contribute to the normalization of sLN$_v$ architecture. In fact, the dFMRP N-terminal region specifically interacts with CYFIP, cooperatively regulating sLN$_v$ axonal projections and synaptic development (Reeve et al., 2008). Thus, we posit that the temporally-specific regulation of these cytoskeleton-modifying dFMRP targets is fundamentally important in establishing and/or maintaining proper synaptic connections within the clock circuit.

The PDF cells have been described as "GABA-responsive wake-promoting" neurons in the clock circuit (Parisky et al., 2008). Suppression of neuronal activity in these cells increases sleep, while coordinately increasing LN$_v$ excitability decreases sleep. sLN$_v$s express the *Rdl* GABA$_A$ receptor, and sLN$_v$-specific *Rdl* knockdown impairs sleep while *Rdl* over-expression yields more rapid sleep onset and enhanced sleep (Parisky et al., 2008). These findings are particularly relevant to the *Drosophila* FraX model, as it has been recently reported that *dfmr1* nulls display increased sleep, while dFMRP over-expression decreases sleep (Bushey et al., 2009). However, *dfmr1* nulls have been shown to under express all known *Drosophila* GABA$_A$ receptor subunits (D'Hulst et al., 2006). Consistently, the *Fmr1* mutant mouse has reduced GABA$_A$ receptors (D'Hulst et al., 2006; Gantois et al., 2006), associated with both structural and functional alterations of the GABAergic circuits in the neocortex and hippocampus, respectively (D'Antuono et al., 2003; Selby et al., 2007). These changes may correlate with recent accounts of neuronal hyperexcitability in both *Drosophila* and mouse FraX models (Gibson et al., 2008; Repicky and Broadie, 2009). A small molecule screen for rescue of *dfmr1*-mutant phenotypes identified GABA, nipecotic acid (GABA reuptake inhibitor) and creatinine (suspected GABA$_A$ receptor activator), again implicating GABAergic signaling (Chang et al., 2008). In *dfmr1* nulls, GABA treatment specifically relieved misregulation of the MAP1B homolog, Futsch, mushroom body β-lobe midline crossing and courtship defects. Together, these data suggest that manipulation of GABA signaling

REFERENCES

Bassell, G. J., and Warren, S. T. (2008). Fragile X syndrome: loss of local mRNA regulation alters synaptic development and function. *Neuron* 60, 201–214.

Bechara, E. G., Didiot, M. C., Melko, M., Davidovic, L., Bensaid, M., Martin, P., Castets, M., Pognonec, P., Khandjian, E. W., Moine, H., and Bardoni, B. (2009). A novel function for fragile X mental retardation protein in translational activation. *PLoS Biol.* 7, e16.

Bolduc, F. V., Bell, K., Cox, H., Broadie, K. S., and Tully, T. (2008). Excess protein synthesis in *Drosophila* fragile X mutants impairs long-term memory. *Nat. Neurosci.* 11, 1143–1145.

Bureau, I., Shepherd, G. M., and Svoboda, K. (2008). Circuit and plasticity defects in the developing somatosensory cortex of FMR1 knock-out mice. *J. Neurosci.* 28, 5178–5188.

Bushey, D., Tononi, G., and Cirelli, C. (2009). The *Drosophila* fragile X mental retardation gene regulates sleep need. *J. Neurosci.* 29, 1948–1961.

Castets, M., Schaeffer, C., Bechara, E., Schenck, A., Khandjian, E. W., Luche, S., Moine, H., Rabilloud, T., Mandel, J. L., and Bardoni, B. (2005). FMRP interferes with the Rac1 pathway and controls actin cytoskeleton dynamics in murine fibroblasts. *Hum. Mol. Genet.* 14, 835–844.

Chang, D. C. (2006). Neural circuits underlying circadian behavior in *Drosophila melanogaster*. *Behav. Processes* 71, 211–225.

Chang, S., Bray, S. M., Li, Z., Zarnescu, D. C., He, C., Jin, P., and Warren, S. T. (2008). Identification of small molecules rescuing fragile X syndrome phenotypes in *Drosophila*. *Nat. Chem. Biol.* 4, 256–263.

D'Antuono, M., Merlo, D., and Avoli, M. (2003). Involvement of cholinergic and gabaergic systems in the fragile X knockout mice. *Neuroscience* 119, 9–13.

D'Hulst, C., De Geest, N., Reeve, S. P., Van Dam, D., De Deyn, P. P., Hassan, B. A., and Kooy, R. F. (2006). Decreased expression of the GABAA receptor in fragile X syndrome. *Brain Res.* 1121, 238–245.

Dictenberg, J. B., Swanger, S. A., Antar, L. N., Singer, R. H., and Bassell, G. J. (2008). A direct role for FMRP in activity-dependent dendritic mRNA transport links filopodial-spine morphogenesis to fragile X syndrome. *Dev. Cell* 14, 926–939.

Dockendorff, T. C., Su, H. S., McBride, S. M., Yang, Z., Choi, C. H., Siwicki, K. K., Sehgal, A., and Jongens, T. A. (2002). *Drosophila* lacking dfmr1 activity show defects in circadian output and fail to maintain courtship interest. *Neuron* 34, 973–984.

Elia, M., Ferri, R., Musumeci, S. A., Del Gracco, S., Bottitta, M., Scuderi, C., Miano, G., Panerai, S., Bertrand, T., and Grubar, J. C. (2000). Sleep in subjects with autistic disorder: a neurophysiological and psychological study. *Brain Dev.* 22, 88–92.

Estes, P. S., O'Shea, M., Clasen, S., and Zarnescu, D. C. (2008). Fragile X protein controls the efficacy of mRNA transport in *Drosophila* neurons. *Mol. Cell. Neurosci.* 39, 170–179.

Fernandez, M. P., Berni, J., and Ceriani, M. F. (2008). Circadian remodeling of neuronal circuits involved in rhythmic behavior. *PLoS Biol.* 6, e69.

Galvez, R., and Greenough, W. T. (2005). Sequence of abnormal dendritic spine development in primary somatosensory cortex of a mouse model of the fragile X mental retardation syndrome. *Am. J. Med. Genet.* 135, 155–160.

Gantois, I., Vandesompele, J., Speleman, F., Reyniers, E., D'Hooge, R., Severijnen, L. A., Willemsen, R., Tassone, F., and Kooy, R. F. (2006). Expression profiling suggests underexpression of the GABA(A) receptor subunit delta in the fragile X knockout mouse model. *Neurobiol. Dis.* 21, 346–357.

Gatto, C. L., and Broadie, K. (2008). Temporal requirements of the fragile X mental retardation protein in the regulation of synaptic structure. *Development* 135, 2637–2648.

Gatto, C. L., and Broadie, K. (2009). The fragile X mental retardation protein in circadian rhythmicity and memory consolidation. *Mol. Neurobiol.* 39, 107–129.

Gibson, J. R., Bartley, A. F., Hays, S. A., and Huber, K. M. (2008). Imbalance of neocortical excitation and inhibition and altered UP states reflect network hyperexcitability in the mouse model of fragile X syndrome. *J. Neurophysiol.* 100, 2615–2626.

Gould, E. L., Loesch, D. Z., Martin, M. J., Hagerman, R. J., Armstrong, S. M., and Huggins, R. M. (2000). Melatonin profiles and sleep characteristics in boys with fragile X syndrome: a preliminary study. *Am. J. Med. Genet.* 95, 307–315.

Grima, B., Chelot, E., Xia, R., and Rouyer, F. (2004). Morning and evening peaks of activity rely on different clock neurons of the *Drosophila* brain. *Nature* 431, 869–873.

Hagerman, R. J., Berry-Kravis, E., Kaufmann, W. E., Ono, M. Y., Tartaglia, N., Lachiewicz, A., Kronk, R., Delahunty, C., Hessl, D., Visootsak, J., Picker, J., Gane, L., and Tranfaglia, M. (2009). Advances in the treatment of fragile X syndrome. *Pediatrics* 123, 378–390.

Helfrich-Forster, C. (1995). The period clock gene is expressed in central nervous system neurons which also produce a neuropeptide that reveals the projections of circadian pacemaker cells within the brain of *Drosophila melanogaster*. *Proc. Natl. Acad. Sci. USA* 92, 612–616.

Helfrich-Forster, C. (2005). Neurobiology of the fruit fly's circadian clock. *Genes Brain Behav.* 4, 65–76.

Inoue, S., Shimoda, M., Nishinokubi, I., Siomi, M. C., Okamura, M., Nakamura, A., Kobayashi, S., Ishida, N., and Siomi, H. (2002). A role for the *Drosophila* fragile X-related gene in circadian output. *Curr. Biol.* 12, 1331–1335.

Khandjian, E. W., Fortin, A., Thibodeau, A., Tremblay, S., Cote, F., Devys, D., Mandel, J. L., and Rousseau, F. (1995). A heterogeneous set of FMR1 proteins is widely distributed in mouse tissues and is modulated in cell culture. *Hum. Mol. Genet.* 4, 783–789.

Laggerbauer, B., Ostareck, D., Keidel, E. M., Ostareck-Lederer, A., and Fischer, U. (2001). Evidence that fragile X mental retardation protein is a negative regulator of translation. *Hum. Mol. Genet.* 10, 329–338.

Larson, J., Jessen, R. E., Kim, D., Fine, A. K., and du Hoffmann, J. (2005). Age-dependent and selective impairment of long-term potentiation in the anterior piriform cortex of mice lacking the fragile X mental retardation protein. *J. Neurosci.* 25, 9460–9469.

Le Clainche, C., and Carlier, M. F. (2008). Regulation of actin assembly associated with protrusion and adhesion in cell migration. *Physiol. Rev.* 88, 489–513.

Lee, A., Li, W., Xu, K., Bogert, B. A., Su, K., and Gao, F. B. (2003). Control of dendritic development by the *Drosophila* fragile X-related gene involves the small GTPase Rac1. *Development* 130, 5543–5552.

Li, Z., Zhang, Y., Ku, L., Wilkinson, K. D., Warren, S. T., and Feng, Y. (2001). The fragile X mental retardation protein inhibits translation via interacting with mRNA. *Nucleic Acids Res.* 29, 2276–2283.

Lu, R., Wang, H., Liang, Z., Ku, L., O'Donnell, W. T., Li, W., Warren, S. T., and Feng, Y. (2004). The fragile X protein controls microtubule-associated protein 1B translation and microtubule stability in brain neuron development. *Proc. Natl. Acad. Sci. USA* 101, 15201–15206.

McBride, S. M., Choi, C. H., Wang, Y., Liebelt, D., Braunstein, E., Ferreiro, D., Sehgal, A., Siwicki, K. K., Dockendorff, T. C., Nguyen, H. T., McDonald, T. V., and Jongens, T. A. (2005). Pharmacological rescue of synaptic plasticity, courtship behavior, and mushroom body defects in a *Drosophila* model of fragile X syndrome. *Neuron* 45, 753–764.

Miano, S., Bruni, O., Elia, M., Scifo, L., Smerieri, A., Trovato, A., Verrillo, E., Terzano, M. G., and Ferri, R. (2008).

Sleep phenotypes of intellectual disability: a polysomnographic evaluation in subjects with Down syndrome and Fragile-X syndrome. *Clin. Neurophysiol.* 119, 1242–1247.

Morales, J., Hiesinger, P. R., Schroeder, A. J., Kume, K., Verstreken, P., Jackson, F. R., Nelson, D. L., and Hassan, B. A. (2002). *Drosophila* fragile X protein, DFXR, regulates neuronal morphology and function in the brain. *Neuron* 34, 961–972.

Nimchinsky, E. A., Oberlander, A. M., and Svoboda, K. (2001). Abnormal development of dendritic spines in FMR1 knock-out mice. *J. Neurosci.* 21, 5139–5146.

Nitabach, M. N., and Taghert, P. H. (2008). Organization of the *Drosophila* circadian control circuit. *Curr. Biol.* 18, R84–R93.

Nitabach, M. N., Wu, Y., Sheeba, V., Lemon, W. C., Strumbos, J., Zelensky, P. K., White, B. H., and Holmes, T. C. (2006). Electrical hyperexcitation of lateral ventral pacemaker neurons desynchronizes downstream circadian oscillators in the fly circadian circuit and induces multiple behavioral periods. *J. Neurosci.* 26, 479–489.

Osterwalder, T., Yoon, K. S., White, B. H., and Keshishian, H. (2001). A conditional tissue-specific transgene expression system using inducible GAL4. *Proc. Natl. Acad. Sci. USA* 98, 12596–12601.

Pan, L., Woodruff, E. III, Liang, P., and Broadie, K. (2008). Mechanistic relationships between *Drosophila* fragile X mental retardation protein and metabotropic glutamate receptor A signaling. *Mol. Cell. Neurosci.* 37, 747–760.

Pan, L., Zhang, Y. Q., Woodruff, E., and Broadie, K. (2004). The *Drosophila* fragile X gene negatively regulates neuronal elaboration and synaptic differentiation. *Curr. Biol.* 14, 1863–1870.

Parisky, K. M., Agosto, J., Pulver, S. R., Shang, Y., Kuklin, E., Hodge, J. J., Kang, K., Liu, X., Garrity, P. A., Rosbash, M., and Griffith, L. C. (2008). PDF cells are a GABA-responsive wake-promoting component of the *Drosophila* sleep circuit. *Neuron* 60, 672–682.

Qin, M., Kang, J., Burlin, T. V., Jiang, C., and Smith, C. B. (2005). Postadolescent changes in regional cerebral protein synthesis: an in vivo study in the FMR1 null mouse. *J. Neurosci.* 25, 5087–5095.

Reeve, S. P., Bassetto, L., Genova, G. K., Kleyner, Y., Leyssen, M., Jackson, F. R., and Hassan, B. A. (2005). The *Drosophila* fragile X mental retardation protein controls actin dynamics by directly regulating profilin in the brain. *Curr. Biol.* 15, 1156–1163.

Reeve, S. P., Lin, X., Sahin, B. H., Jiang, F., Yao, A., Liu, Z., Zhi, H., Broadie, K., Li, W., Giangrande, A., Hassan, B. A., and Zhang, Y. Q. (2008). Mutational analysis establishes a critical role for the N terminus of fragile X mental retardation protein FMRP. *J. Neurosci.* 28, 3221–3226.

Renn, S. C., Park, J. H., Rosbash, M., Hall, J. C., and Taghert, P. H. (1999). A pdf neuropeptide gene mutation and ablation of PDF neurons each cause severe abnormalities of behavioral circadian rhythms in *Drosophila*. *Cell* 99, 791–802.

Repicky, S. E., and Broadie, K. (2009). Metabotropic glutamate receptor mediated use-dependent down-regulation of synaptic excitability involves the fragile X mental retardation protein. *J. Neurophysiol.* 101, 672–687.

Roman, G., Endo, K., Zong, L., and Davis, R. L. (2001). P[Switch], a system for spatial and temporal control of gene expression in *Drosophila melanogaster*. *Proc. Natl. Acad. Sci. USA* 98, 12602–12607.

Schenck, A., Bardoni, B., Langmann, C., Harden, N., Mandel, J. L., and Giangrande, A. (2003). CYFIP/Sra-1 controls neuronal connectivity in *Drosophila* and links the Rac1 GTPase pathway to the fragile X protein. *Neuron* 38, 887–898.

Sekine, T., Yamaguchi, T., Hamano, K., Siomi, H., Saez, L., Ishida, N., and Shimoda, M. (2008). Circadian phenotypes of *Drosophila* fragile x mutants in alternative genetic backgrounds. *Zoolog. Sci.* 25, 561–571.

Selby, L., Zhang, C., and Sun, Q. Q. (2007). Major defects in neocortical GABAergic inhibitory circuits in mice lacking the fragile X mental retardation protein. *Neurosci. Lett.* 412, 227–232.

Sheeba, V., Sharma, V. K., Gu, H., Chou, Y T., O'Dowd, D. K., and Holmes, T. C. (2008). Pigment dispersing factor-dependent and -independent circadian locomotor behavioral rhythms. *J. Neurosci.* 28, 217–227.

Singh, K., Gaur, P., and Prasad, S. (2007). Fragile X mental retardation (Fmr-1) gene expression is down regulated in brain of mice during aging. *Mol. Biol. Rep.* 34, 173–181.

Singh, K., and Prasad, S. (2008). Differential expression of Fmr-1 mRNA and FMRP in female mice brain during aging. *Mol. Biol. Rep.* 35, 677–684.

Siomi, M. C., Siomi, H., Sauer, W. H., Srinivasan, S., Nussbaum, R. L., and Dreyfuss, G. (1995). FXR1, an autosomal homolog of the fragile X mental retardation gene. *EMBO J.* 14, 2401–2408.

Stoleru, D., Peng, Y., Agosto, J., and Rosbash, M. (2004). Coupled oscillators control morning and evening locomotor behaviour of *Drosophila*. *Nature* 431, 862–868.

Sung, Y. J., Dolzhanskaya, N., Nolin, S. L., Brown, T., Currie, J. R., and Denman, R. B. (2003). The fragile X mental retardation protein FMRP binds elongation factor 1A mRNA and negatively regulates its translation in vivo. *J. Biol. Chem.* 278, 15669–15678.

Tessier, C. R., and Broadie, K. (2008). *Drosophila* fragile X mental retardation protein developmentally regulates activity-dependent axon pruning. *Development* 135, 1547–1557.

Wu, Y., Cao, G., Pavlicek, B., Luo, X., and Nitabach, M. N. (2008). Phase coupling of a circadian neuropeptide with rest/activity rhythms detected using a membrane-tethered spider toxin. *PLoS Biol.* 6, e273.

Yoshii, T., Wulbeck, C., Sehadova, H., Veleri, S., Bichler, D., Stanewsky, R., and Helfrich-Forster, C. (2009). The neuropeptide pigment-dispersing factor adjusts period and phase of *Drosophila*'s clock. *J. Neurosci.* 29, 2597–2610.

Yun, S. W., Platholi, J., Flaherty, M. S., Fu, W., Kottmann, A. H., and Toth, M. (2006). Fmrp is required for the establishment of the startle response during the critical period of auditory development. *Brain Res.* 1110, 159–165.

Zalfa, F., Adinolfi, S., Napoli, I., Kuhn-Holsken, E., Urlaub, H., Achsel, T., Pastore, A., and Bagni, C. (2005). Fragile X mental retardation protein (FMRP) binds specifically to the brain cytoplasmic RNAs BC1/BC200 via a novel RNA-binding motif. *J. Biol. Chem.* 280, 33403–33410.

Zalfa, F., Giorgi, M., Primerano, B., Moro, A., Di Penta, A., Reis, S., Oostra, B., and Bagni, C. (2003). The fragile X syndrome protein FMRP associates with BC1 RNA and regulates the translation of specific mRNAs at synapses. *Cell* 112, 317–327.

Zhang, J., Fang, Z., Jud, C., Vansteensel, M. J., Kaasik, K., Lee, C. C., Albrecht, U., Tamanini, F., Meijer, J. H., Oostra, B. A., and Nelson, D. L. (2008). Fragile X-related proteins regulate mammalian circadian behavioral rhythms. *Am. J. Hum. Genet.* 83, 43–52.

Zhang, M., Wang, Q., and Huang, Y. (2007). Fragile X mental retardation protein FMRP and the RNA export factor NXF2 associate with and destabilize Nxf1 mRNA in neuronal cells. *Proc. Natl. Acad. Sci. USA* 104, 10057–10062.

Zhang, Y., O'Connor, J. P., Siomi, M. C., Srinivasan, S., Dutra, A., Nussbaum, R. L., and Dreyfuss, G. (1995). The fragile X mental retardation syndrome protein interacts with novel homologs FXR1 and FXR2. *EMBO J.* 14, 5358–5366.

Zhang, Y. Q., Bailey, A. M., Matthies, H. J., Renden, R. B., Smith, M. A., Speese, S. D., Rubin, G. M., and Broadie, K. (2001). *Drosophila* fragile X-related gene regulates the MAP1B homolog Futsch to control synaptic structure and function. *Cell* 107, 591–603.

Zhang, Y. Q., Rodesch, C. K., and Broadie, K. (2002). Living synaptic vesicle marker: synaptotagmin-GFP. *Genesis* 34, 142–145.